Available online at www.sciencedirect.com
SCIENCE DIRECT
Polymer 46 (2005) 2955–2965
polymer
www.elsevier.com/locate/polymer

Confined crystallization phenomena in immiscible polymer blends with dispersed micro- and nanometer sized PA6 droplets, part 3: crystallization kinetics and crystallinity of micro- and nanometer sized PA6 droplets crystallizing at high supercoolings

R.T. Tol, V.B.F. Mathot, G. Groeninckx*

Laboratory of Macromolecular Structural Chemistry, Division of Polymer Chemistry, Department of Chemistry, Catholic University of Leuven, Celestijnenlaan 200F, B-3001 Heverlee, Belgium

Received 24 June 2004; received in revised form 16 November 2004; accepted 1 February 2005
Available online 26 February 2005

Abstract

Crystallization kinetics and crystallinity development of PA6 droplets having sizes from 0.1 to 20 μm dispersed in immiscible uncompatibilized PS/PA6 and reactively compatibilized (PS/Styrene-maleic anhydride copolymer = SMA2)/PA6 blends are reported. These blend systems show fractionated crystallization, leading to several separate crystallization events at different lowered temperatures. Isothermal DSC experiments show that micrometer-sized PA6 droplets crystallizing in an intermediate temperature range ($T_c \sim 175$ °C) below the bulk crystallization show a different dependency on cooling rate compared to bulk crystallization, and an athermal crystallization mechanism is suggested for PA6 in this crystallization temperature region. The crystallinity in these blends decreases with PA6 droplet size. Random nucleation, characteristic for a homogeneous nucleation process, is found for sub-micrometer sized PA6 droplets crystallizing between T_c 85 and 110 °C using isothermal DSC experiments. However, crystallization in the PA6 droplets is most likely initiated at the PA6-PS interface due to vitrification of the PS matrix during crystallization. Very imperfect PA6 crystals are formed in this low temperature crystallization region, leading to a strongly reduced crystallinity. These crystals show strong reorganization effects upon heating.

Keywords: Confined crystallization; Homogeneous nucleation; Crystallinity

1. Introduction

When a crystallizable polymer is isolated in a confining volume, its crystallization behavior can be drastically changed compared to its bulk crystallization. In immiscible blends, where the confinement is brought about by the fine dispersion of crystallizable droplets inside a polymer matrix, several crystallization events at different, lowered crystallization temperatures can be observed [1–7]. The main reason for this so-called 'fractionated crystallization' phenomenon was found to be the lack of active heterogeneities in the isolated droplets. The spectrum of supercoolings obtained upon cooling reflects the difference in nucleating activity of various heterogeneities in the melt, present in the dispersed droplets [1]. This crystallization phenomenon can in fact be viewed as a quite general crystallization mechanism for crystallization in dispersions, because basically similar observations have been made for liquid emulsions [8–10] and metals [11,12]. It is observed in various polymer systems, when the polymer is present in a confined, isolated state, i.e. copolymers with nanometer sized crystallizable domains obtained via micro-phase separation and dispersions of polymers using a solvent or oil. [13–29].

When the available heterogeneities are confined to a small portion of the droplets, the remaining heterogeneity-free droplets are forced to nucleate at rates governed by the molecular characteristics of the sample. Therefore, in the extreme, crystallization will occur via homogeneous nucleation, which will generally require the highest supercooling for crystallization because of the higher activation energy needed for chain association in the absence of a

* Corresponding author. Tel.: +32 16 327440; fax: +32 16 327990.
E-mail address: gabriel.groeninckx@chem.kuleuven.ac.be (G. Groeninckx).

0032-3861/$ - see front matter © 2005 Elsevier Ltd. All rights reserved.
doi:10.1016/j.polymer.2005.02.020

nucleating substrate. This is the reason why in a number of studies on dispersed droplet systems, the lowest crystallization temperature obtained is usually connected to homogeneous nucleation [2,4,14,20,30]. Obviously, this is necessary but not sufficient to prove homogeneous nucleation. The mechanism of homogeneous nucleation is expected to proceed totally differently from a heterogeneous one. Instead of nucleation predetermined by the present heterogeneous nucleation sites, homogeneous nucleation is a random process of associations of chains (segments).

The interest in the crystallization kinetics of confined, supercooled polymers is steadily increasing [16–19,22,23,31]. Random nucleation, characteristic for homogeneous nucleation, was found in various confined systems using optical microscopy [27,29], dilatometry [13], DSC [18,23] or real-time SAXS/WAXD experiments [16,17,19]. In a number of cases a strong temperature dependence was found for the confined, supercooled polymer [16–18,32]. Reiter et al. [22] were able to directly visualize independent, random crystallization of nano-compartments of PEO, by using real-time AFM measurements. For immiscible polymer blends with small crystallizable droplets, however, a detailed kinetic study has never been performed.

Fractionated crystallization and homogeneous nucleation can be expected to have important consequences for the final semicrystalline structure of the confined polymer. Several authors report a drop in the degree of crystallinity upon fractionated crystallization, both in immiscible blends [2,5,30,32–34] as well as for the confined crystallization of micro-phase separated domains in crystallizable block copolymers [13–15]. In most cases it is assumed that the decrease of crystallinity can be attributed to the formation of thinner and less perfect crystalline structures at higher degrees of supercooling. Everaert et al. [34] have recently obtained interesting results using time-resolved SAXS/WAXD experiments on a blend system where POM was finely dispersed in a PPE/PS matrix. From the evolution of the lamellar crystal thickness with crystallinity, it was found, in addition, that also the lateral dimensions of the crystallites were found to be affected, which in the case of small crystallizing droplets were stated to be limited by the size of the droplets. These observations indicate the important effects of confinement on the resulting semicrystalline structure, with respect to the dimensions of the crystallites and their low crystallization temperatures.

In two earlier publications [5,6] we reported on the fractionated crystallization phenomena when PA6 was dispersed as (sub)-micrometer sized domains in immiscible blends with PS or PPE/PS as matrix. In these reports, it has been shown that a broad range of crystallization temperatures could be obtained for PA6, mainly via adjusting the blend morphology. For uncompatibilized immiscible blends with micrometer-sized PA6 droplets, crystallization mainly took place at intermediate temperatures [5]. For the same immiscible blends, reactively compatibilized with styrene-maleic anhydride (SMA) copolymers, PA6 droplet sizes in the sub-micrometer range were generated and very low crystallization temperatures were obtained [6].

In this paper, uncompatibilized PS/PA6 blends as well as blends reactively compatibilized with SMA2 (SMA with 2 wt% anhydride functionalities) will be investigated. The phase morphology and rheology of these blend systems were described in detail in a previous publication [35]. These blend systems cover a broad range of both PA6 droplet sizes (between 0.1 and 20 μm) as well as PA6 crystallization temperatures (between 80 and 185 °C). As such, these blends form interesting model systems to study crystallization kinetics and crystallinity changes over a very broad temperature range, using normal thermal histories, e.g. without the need to use high cooling rates. Thus it is possible to do so at both intermediate as well as low crystallization temperatures by performing isothermal DSC experiments. In addition, the crystallinity of the PA6 in the sub-micrometer sized droplets crystallizing at different temperatures is investigated via DSC experiments.

2. Materials and methods

2.1. Materials, preparation and phase morphology characterization

Polyamide-6 (PA Akulon K123) was provided by DSM Research, Geleen, The Netherlands. Atactic polystyrene (PS Styron E680) was supplied by DOW Benelux, Terneuzen, The Netherlands. The miscible polyphenylene-ether/polystyrene (PPE/PS) 50/50 wt/wt mixture was prepared by mixing polyphenylene-ether (PPE) (supplied by GE Plastics, Bergen op Zoom, The Netherlands) and PS (supplied by DOW) in a Haake Rheocord 90 twin-screw extruder [36]. Styrene-maleic anhydride copolymer SMA2 (SEA 0579) was provided by Bayer, Dormagen, Germany. PS and (PPE/PS) 50/50 wt/wt are miscible with SMA2 over the whole composition range [37,38]. The number after SMA denotes the wt% maleic anhydride in SMA.

Two-phase PS/PA6, (PS/SMA2)/PA6 and (PPE/PS/SMA2)/PA6 blends were prepared on a co-rotating twin-screw mini-extruder manufactured by DSM Research, Geleen, The Netherlands. A complete description of the material characteristics and processing conditions can be found in a previous paper [35]. In most of these blend systems, PA6 formed droplets inside the amorphous matrix. Averages and distributions of PA6 droplet sizes were obtained using image analysis of SEM pictures, of which a detailed description is presented in [35].

2.2. Thermal analysis

2.2.1. Dynamic and isothermal crystallization experiments

Dynamic and isothermal DSC measurements were

performed using a Perkin Elmer Pyris 1. Dynamic means here that temperature was varied at a constant rate. The nitrogen flow-rate was 20 ml/min. Temperature and enthalpy calibration were performed with indium (T_m = 156.6 °C) and tin (T_m = 231.88 °C) at a heating rate of 10 K/min. Furnace calibration was performed between 0 and 290 °C. The samples were first heated at a rate of 40 K/min to a melt temperature of 260 °C, and kept there for 3 min in order to erase all thermal history. It was observed that this procedure was sufficient to avoid self-nucleation. Then, the samples were cooled at 10 K/min to 25 °C. Subsequent melting scans were performed at a rate of 10 K/min. Sample masses of about 5 mg were used in case of scan rates of 10 K/min. Weighing was done using an AND Hm-202 balance with an accuracy of 0.01 mg. Sample masses were adjusted according to the applied cooling rate (approximately 5 mg for 10 K/min; ~10 mg for 1 K/min and ~20 mg for 0.1 K/min). DSC curves were corrected for instrumental curvature by subtracting empty-pan curves, measured using identical thermal histories at the beginning and end of each day.

For the isothermal crystallization measurements, the sample was heated at a rate of 40 K/min to a melt temperature of 260 °C, and kept there for 3 min, similar to the dynamic experiments. In the second step the sample was cooled down to the isothermal crystallization temperature T_{iso} at a rate of 10 K/min. The sample was held at the chosen isothermal crystallization temperature for times varying between 0 and 240 min. The melting area for t_{iso} = 0 s was subtracted from each consecutive isothermal experiment. After each isothermal crystallization time interval, the melting behavior was recorded at a heating rate of 10 K/min. The melting peak area was determined from about 130 to 230 °C for low isothermal crystallization temperatures (~100 °C) and from about 180 to 230 °C for intermediate crystallization temperatures (~175 °C). In this way we correct for possible reorganization or cold crystallization during the heating run. A normal calibration set-up at 10 K/min heating rate was used for calibration but the isothermal temperature was each time set corresponding to the real sample (sensor) temperature (instead of the DSC program temperature).

The mass fraction crystallinity of PA6 in the blends was calculated using temperature dependent Δh values for fully amorphous and fully crystalline PA6 available from the ATHAS databank [39] via:

$$\omega_c(T) = \frac{\Delta h\,\exp(T)}{\Delta h(T)} \tag{1}$$

with $\Delta h(T) = h_a(T) - h_c(T)$, the difference between the enthalpy at T of fully amorphous and fully crystalline PA6, respectively.

In case of calculating the crystallinity from the melting peak, T was taken equal to $T_{m(peak\ max)}$ and recrystallization exotherms were subtracted for calculating Δh_mexp. For calculating crystallinity from the crystallization curve, T was taken equal to $T_{c(peak\ max)}$. The following addition was used in case of different crystallization peaks.

$$\omega_c = \frac{\Delta h\,\exp(T_1)}{\Delta h(T_1)} + \frac{\Delta h\,\exp(T_2)}{\Delta h(T_2)} + \cdots \tag{2}$$

For this calculation the denominator of Eq. (1), $\Delta h(T)$, for the monoclinic γ phase of PA6 was taken equal to that one of the monoclinic α phase of PA6. This is justified by literature data: $\Delta h(T_m^\circ)_{\alpha\ phase}$ = 230 J/g [40] and $\Delta h(T_m^\circ)_{\gamma\ phase}$ = 239 J/g [41].

2.2.2. Self-nucleation experiments

Self-nucleation experiments were also performed using the Pyris 1 DSC. With this method the nucleation density is increased enormously by heating up the material within the self-nucleation regimes where small crystal residues are still present in the melt [42].

The following procedure was applied in this investigation:

Step 1 Erasing thermal history and creating a initial standard state. The samples were first heated to 260 °C at 40 K/min, and kept there for a 3 min isothermal period. Subsequently, the samples were cooled to room temperature at a cooling rate of 10 K/min.

Step 2 Heating to T_s (Self-nucleation temperature), situated between 220 and 260 °C, at a heating rate of 10 K/min.

If T_s is 260 °C or higher, the sample is said to be in domain I, where complete melting is realized. When T_s is high enough to melt the material almost completely, but low enough to leave small crystal fragments capable of acting as self-nuclei, this is domain II, the self-nucleation region. When T_s is too low, only part of the crystals will be melted, and quite some remaining crystals will be annealed at T_s. This is domain III, giving rise to both self-nucleation and annealing.

Step 3 Isothermal conditioning at T_s during 3 min.

Step 4 Crystallization at a cooling rate of 10 K/min from T_s to room temperature.

Step 5 Melting after crystallization at a heating rate of 10 K/min.

3. Results and discussion

3.1. Crystallization of PA6 at intermediate supercooling

In a previous paper [5] it was found that dispersing of PA6 to droplet sizes of about 1–10 μm in a PS matrix, resulted in fractionated crystallization, causing a second PA6 crystallization peak around 170 °C, about 15 °C lower

than the PA6 bulk crystallization temperature. It was also observed that the number of crystallization peaks was independent of the cooling rate, with the exception of very high cooling rates leading to an overlap of peaks. Interestingly, however, the intermediate PA6 crystallization peak temperature was clearly less dependent on the applied DSC cooling rate than the normal bulk crystallization peak temperature. This observation may be point to a different crystallization mechanism for PA6 at lower crystallization temperatures.

Therefore, isothermal DSC measurements have been used to study the PA6 crystallization kinetics at these intermediate crystallization temperatures. Note that we refer to intermediate crystallization peaks, because of the presence of peak at even lower crystallization temperatures upon lowering the PA6 droplet size further via reactive compatibilization (see Section 3.2). To determine the crystallization half time for the second, intermediate temperature crystallization peak, the PS/PA6 85/15 blend composition was chosen. For this blend, only a very small fraction of the PA6 crystallizes at the bulk temperature, which facilitates the direct observation of the intermediate crystallization temperature, without interference of the bulk crystallization. Morphological and thermal data of this 85/15 blend composition have been indicated in Table 1. After the standard DSC heating treatment, the blend was cooled at a rate of 10 K/min to different isothermal temperatures. However, isothermal crystallization at temperatures from 190 °C down to 174 °C, the latter being the onset for dynamic crystallization of the intermediate crystallization peak at 10 K/min cooling rate (see Table 1), did not result in a measurable crystallization signal with time. Increasing the cooling rate to T_{iso} to 150 K/min, followed by isothermal crystallization close to the onset of dynamic crystallization (for a cooling rate of 150 K/min), did not improve the crystallization signal.

To be able to follow the amount of crystallized material during isothermal crystallization, the DSC curves of melting after isothermal crystallization were used. After the standard thermal treatment, the PS/PA6 85/15 sample was cooled down to T_{iso} at a cooling rate of 10 K/min. For cooling at a rate of 10 K/min, the onset for crystallization is situated around 175 °C. For this experiment temperatures T_{iso} of 180, 178, and 176 °C were used, so no crystallization occurred upon cooling to T_{iso}. Fig. 1 shows the evolution of the melting enthalpy of the PS/PA6 85/15 blend after isothermal crystallization as a function of crystallization time at the different isothermal crystallization temperatures. It can be seen from this figure that the evolution of the melting enthalpy versus time is the same for the three applied crystallization temperatures. First, a steep increase in melting enthalpy is observed during the first few minutes of crystallization. At intermediate times (between 6 and 10 min), a slight decrease in enthalpy is observed. At long crystallization times, the melting enthalpy increases further. The melting enthalpy shows a very strong dependence on the crystallization temperature. Lowering the crystallization temperature drastically increases the amount of crystallized material. Interestingly, the melting enthalpies at the different crystallization temperatures do not reach the same value as obtained after dynamic cooling. This is contrary to the situation for bulk crystallization of PA6, for which isothermal crystallization at different temperatures will yield the same final value when all material has been crystallized. Also, the crystallization enthalpy after isothermal crystallization is close to the crystallization enthalpy from dynamic cooling experiments. Comparing the final values of the melting enthalpies in Fig. 1 with the final value obtained after dynamic cooling, which is 51 J/g_{PA6} (see Table 1), one observes that the melting enthalpy after these isothermal crystallization temperatures is still much lower than that after dynamic crystallization. The remaining nuclei in the droplets thus seem to become active at specific temperatures, drastically increasing the amount of active nuclei upon lowering the temperature, making the subsequent melting enthalpy strongly dependent on the crystallization temperature.

This type of behavior could be explained by assuming an athermal nucleation mode at lower crystallization temperatures. For PA6 bulk crystallization, the crystallization normally can be described by a thermal heterogeneous nucleation mechanism, where new crystals start growing throughout the cooling [43]. For athermal nucleation, all crystals start growing at the same time at a specific temperature. A study of Janeschitz-Kriegl et al. [44], suggests that the number of athermal nuclei is likely to increase remarkably at lower temperatures, once all thermal nuclei have been exhausted. Once nucleation starts—within a very specific temperature range—the crystals start to grow, probably at quite a high rate. The suggested athermal nucleation mechanism can explain the much stronger sensitivity of the PA6 bulk peak (thermal nucleation) to the cooling rate compared to the lower temperature peak.

A prediction of the spherulitic growth rate as a function of crystallization temperature can be done using the dimensionless master curve of growth rate of Gandica and

Table 1
Thermal properties of PA6 and a PS/PA6 85/15 blend

Sample	$D_{n\ PA6}$ (μm)	(D_v/D_n) (−)	$T_{c,peak\ (bulk)}$ (°C)	$T_{c,\ onset\ (bulk)\ @\ 10\ K/min}$ (°C)	$T_{c,\ peak\ (peak\ 2)}$ (°C)	$T_{c,\ onset\ (peak\ 2)}$ (°C)	$\Delta h_{c\ (bulk)}$ (J/g_{PA6})	$\Delta h_{c\ (peak\ 2)}$ (J/g_{PA6})
PA6	–	–	189	195	–	–	77	–
PS/PA6 85/15	1.4	1.6	188	193	169	174	2	51

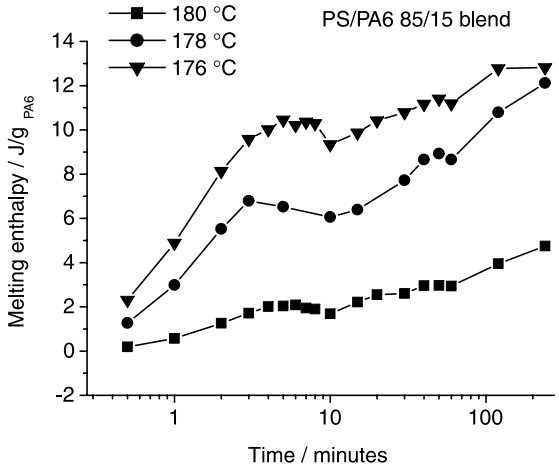

Fig. 1. Melting enthalpy of PA6 in a PS/PA6 85/15 blend as function of crystallization time at 180, 178 and 176 °C.

Magill [45]. In this curve the ratio v/v_{max} is plotted versus a dimensionless crystallization temperature:

$$\theta = \frac{T - T_\infty}{T_m - T_\infty} \tag{3}$$

where $T_\infty \sim (T_g - 50)$ and T_m the experimental melting temperature.

For PA6: $T_g = 50$ °C, $T_m = 221$ °C: a value for T_c, corresponding to the temperature of maximum rate of growth, of 135 °C is obtained. This value coincides very well with the experimentally determined maximum of PA6 growth rate [46]. All crystallization for the PS/PA6 blends thus takes place at the high temperature side of this bell-shaped curve, implying a fast increase of the spherulitic growth rate with decreasing crystallization temperature. Calculating the v/v_{max} ratio for both crystallization temperatures, 185 and 170 °C, using the dimensionless temperature, a very strong increase of the spherulitic growth rate is estimated upon lowering T_c from 185 to 170 °C. An estimation of the (maximum) overall crystallization rate during isothermal crystallization of PS/PA6 85/15 can be obtained by calculating the time to reach 50% of the melting enthalpy during the first steep increase. This time varied between 1 and 2 min for the three different temperatures (and even somewhat longer for $T_{iso} = 176$ °C), which values are only just lower than the crystallization half-time for PA6 crystallization at 195 °C ($t_{1/2} \sim 120$ s, see Fig. 5). Apparently, the overall crystallization rate is not strongly increasing at lower crystallization temperatures for these droplet morphologies.

3.2. Crystallization kinetics of PA6 at high supercooling

3.2.1. Homogeneous nucleation kinetics via isothermal crystallization experiments

As discussed in a previous paper [6], crystallization of the sub-micrometer PA6 droplets resulting after reactive compatibilization of the PS/PA6 blend with SMA2 causes a shift in crystallization temperature to as low as 85 °C, more than 100 °C lower than the PA6 bulk crystallization temperature, caused by the lack of heterogeneous nuclei inside the small PA6 droplets.

In Fig. 2 the position of this low temperature PA6 crystallization peak is plotted as a function of the DSC cooling rate. Obviously, the dependence of the low crystallization peak temperature on the applied DSC cooling rate is quite comparable to that of the PA6 bulk crystallization; the independency of the crystallization peak on the applied cooling rate as found for the droplets crystallized at intermediate temperatures [5] is clearly not found in this temperature range.

For the (PS/SMA2)/PA6 blends studied, again it appears to be impossible to measure a significant exothermic signal during isothermal crystallization experiments, as was the case for PS/PA6 85/15 blend at intermediate supercoolings. Therefore, to study the crystallization kinetics, the evolution of the melting enthalpy of PA6 after isothermal crystallization was investigated. Fig. 3 shows the variation of the melting enthalpy of PA6 as a function of the isothermal crystallization temperature for the (PS/SMA2)/PA6 (62/13)/25 blend after cooling at 150 K/min. It is seen that the melting enthalpy develops steadily from 130 °C down to 104 °C, and increases appreciable with decreasing crystallization temperatures until a final value for the melting enthalpy is reached at 85 °C.

In Fig. 4 the fraction of uncrystallized droplets, derived from the evolution of the melting enthalpy, is plotted as a function of time for three different isothermal crystallization temperatures, after cooling at 10 K/min to T_{iso}. The melting enthalpy after 240 min crystallization was taken as the final value, where all material has crystallized. The lines represent a first order exponential function, showing good agreement up to 120 min for the measured data points at 100 °C and 102 °C, and still reasonable agreement for the 98 °C data. The crystallization of PA6 droplets seems to differ from the sigmoidal kinetics found for bulk

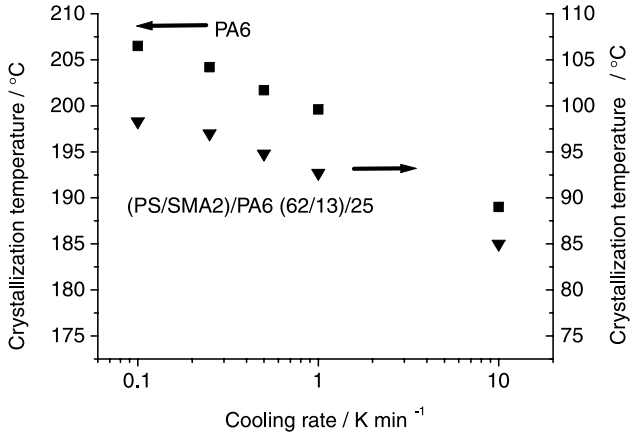

Fig. 2. Crystallization peak temperature as function of cooling rate for PA6 (■) and PA6 in a (PS/SMA2)/PA6 (62/13)/25 blend (▼).

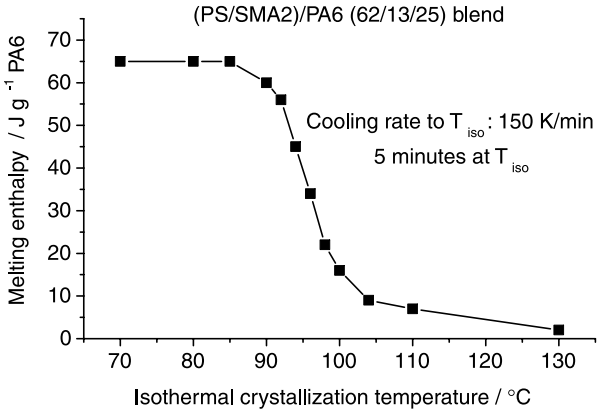

Fig. 3. Melting enthalpy of PA6 in a (PS/SMA2)/PA6 (62/13)/25 blend as a function of isothermal crystallization temperature. Cooling to T_{iso} at 150 K/min $t_{iso}=5$ min.

crystallizing PA6 (see [6]), though the different evaluation procedures make a one-to-one comparison impossible. Similar first order crystallization kinetics as presented here was found in 'droplet' experiments [27], as well as for confined crystallizable micro-phases in block copolymers [16–18,22]. It was related to a different nucleation mechanism at lower crystallization temperatures, most likely a homogeneous nucleation mechanism in the small droplets.

Homogeneous nucleation, by self-association of polymer chain segments, implies that each segment involved crystallizes independently and random in time. The kinetics of random, independent nucleation can be described by [24]:

$$N/N_0 = \exp(-kt) \tag{4}$$

N/N_0 represents the fraction of droplets not yet crystallized and k is a constant.

Plotting log (N/N_0) versus time thus should yield a straight line with slope $-k$. This plot is given in Fig. 4b for the (PS/SMA2)/PA6 (62/13)/25 blend. For the three crystallization temperatures considered a straight line is fitted through the data, which is quite successful for the 100 and 102 °C data, up to 120 min.

The temperature dependence of the crystallization half-time for bulk PA6 and the (PS/SMA2)/PA6 (62/13)/25 blend is given in Fig. 5. This plot shows an order-of-magnitude difference between the crystallization half times of bulk crystallized PA6 and those of PA6 in the (PS/SMA2)/PA6 blend, crystallizing at low temperatures. This explains the impossibility for recording an isothermal crystallization signal for the homogeneous crystallization. Because of the huge amount of droplets that have to be nucleated individually ($>10^{14}$ cm^{-3}), the crystallization is extended over a relatively broad time-interval. Fig. 5 also shows a stronger temperature dependence for the low temperature peak around 100 °C compared to bulk crystallizing PA6. This can be accounted for by comparing the temperature dependence of primary and secondary (growth) nucleation. If the growth is assumed to be instantaneous, only the temperature dependence of primary nucleation is measured for the low temperature crystallization. For bulk crystallizing PA6, the overall crystallization rate is a

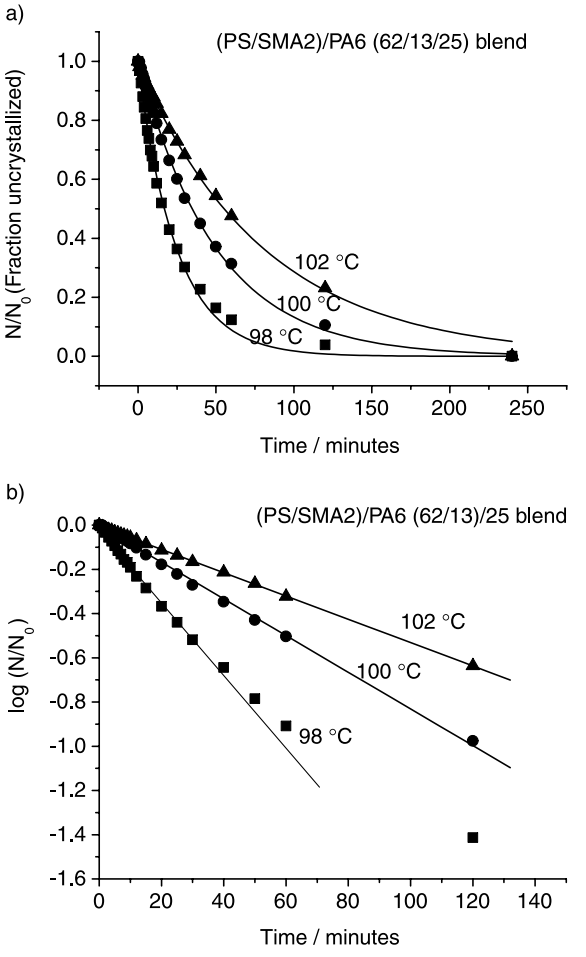

Fig. 4. Fraction (a) and log fraction (b) of uncrystallized droplets (N/N_0) as a function of time for a (PS/SMA2)/PA6 (62/13)/25 blend at different crystallization temperatures. Cooling to T_{iso}: 10 K/min.

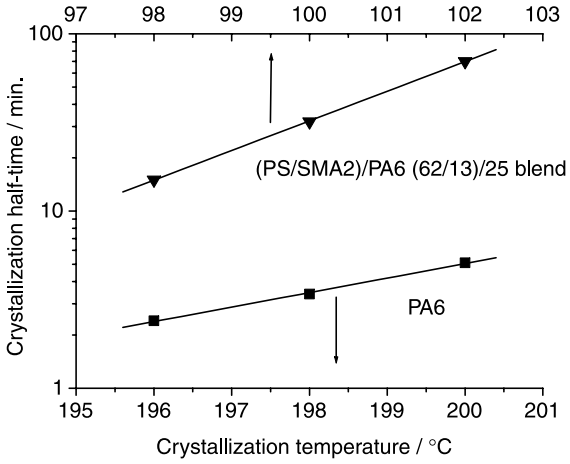

Fig. 5. Crystallization half-time versus isothermal crystallization temperature for PA6 and a (PS/SMA2)/PA6 (62/13)/25 blend.

combination of both primary and secondary nucleation. Secondary nucleation in general is characterized by a less strong temperature dependence compared to primary nucleation [43]. The assumption of a nucleation controlled crystallization in these droplets seems probable, because the lateral crystallite sizes are limited in the 150 nm small PA6 droplets in this investigation. The extremely high nucleation density at these low crystallization temperatures will most likely restrict the lateral growth even further. The growth rate in small droplets was experimentally determined by Barham et al. [29]. The authors found an almost instantaneous growth rate (>2 m/s) in small PE droplets at low crystallization temperatures (supercooling of 40 °C to $T_{c,bulk}$), which was assigned to a regime III crystallization, predicted by Hoffmann for crystallization at high degrees of supercooling [47].

Interestingly, it can be observed that for the (PS/SMA2)/PA6 blends, random nucleation kinetics are observed even at PA6 concentrations as high as 40 wt%, see Table 2. This is, as far as we know, the highest reported volume fraction of crystallizable polymer in an immiscible blend exhibiting such kinetics. This has to be attributed to the effect of the in situ generated compatibilizer, reducing the blend interfacial tension and droplet coalescence, and strongly improving the level of dispersion for high volume fractions of one of the components.

3.2.2. *Effect of droplet size, reactive compatibilizer and droplet interface on the nucleation kinetics*

If true homogeneous volume nucleation occurs, one can also use for Eq. (4) [24,28]:

$$N/N_0 = \exp(-Ivt) \tag{5}$$

where I is the nucleation rate expressed in number of nuclei per unit volume and time, and v is the average volume of the droplet. This means that the nucleation rate can be calculated, when the droplet volume v is known. It is also clear, based on the classical critical size concept for nucleation by Turnbull and Fischer [48], that the chance for nucleation will be affected by the size of the droplets. This is very clearly seen from Fig. 6 where a significant decrease in homogeneous nucleation peak temperature can be found upon decreasing the PA6 droplet size. A similar observation for the shift in homogeneous nucleation temperature with droplet size has been found by Montenegro et al. [10]. Recently, Massa et al. [49] have been able to study homogeneous nucleation of discrete droplets of poly(ethylene oxide) that are formed by the dewetting of a thin film on an unfavourable substrate. In this publication a clear droplet size effect on homogeneous nucleation of micrometer sized PEO droplets was observed.

In such kinetic analysis, the droplet size dispersity is important. The dependence of homogeneous nucleation on the droplet size can lead to serious deviations in kinetic plots (i.e. Fig. 4) for polydisperse samples. The deviation from

Table 2
Morphological and thermal parameters of (PS/SMA2)/PA6 and (PPE/PS/SMA2)/PA6 blend compositions

Blend system	Wt% PA6	D_n PA6 (μm)	(D_v/D_n) (−)	N_v (cm^{-3})	$T_{c,peak}$ (°C)				Δh_c (J/g_{PA6})				Δh_m (J/g_{PA6})	$T_{m,peak}$ (°C)
					1	2	3	4	1	2	3	4		
PA6	100	–	–	–	189	–		–	77	–	–	–	81	221
(PS/SMA2[a])/PA6	25	0.13	1.4	8.4×10^{13}	–	160	–	88	–	1	–	27	62	219
	25[b]	0.11	1.5	1.2×10^{14}	–	159		86	–	0.1	–	29	61	218
	30	0.15	1.4	5.7×10^{13}	–	156	–	89	–	5	–	28	58	219
	35	0.19	1.6	2.2×10^{13}	–	161	–	90	–	6	–	27	57	220
	40	0.29	1.9	5.1×10^{12}	–	162	–	94	–	4	–	30	58	219
(PPE/PS/SMA2[a])/PA6	15[c]	0.09	1.7	8.9×10^{13}	–	150–160	–	83	–	7	–	25	56	218
	20[c]	0.13	1.6	4.2×10^{13}	–	150–160	111	85	–	15	1	13	53	218
	25	0.17	1.8	1×10^{13}	–	150–160	111	85	–	36	1	7	51	218

[a] PS/SMA2 and (PPE/PS)/SMA2 92/8.
[b] PS/SMA2 82/18.
[c] (PPE/PS)/SMA2 95/5.

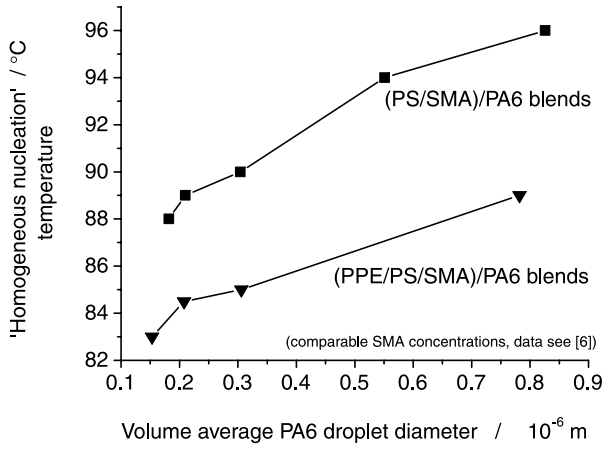

Fig. 6. Homogeneous nucleation temperature as a function of PA6 droplet for (PS/SMA2)/PA6 and (PPE/PS/SMA2)/PA6 blends.

linearity in Fig. 4 for the isothermal temperature of 98 °C can be accounted for by the slower nucleation of the larger droplets, leading to a change in slope at increasing time. Recently, Perepezko et al. [31] have shown that calorimetric measurements provide an effective means to determine the nucleation frequency in droplet samples. They conclude that for the evaluation of the full crystallization kinetics, it is essential to include the droplet size distribution in the analysis.

However, random nucleation as indicated by the kinetic experiments, is not a definite proof for homogeneous nucleation, as already remarked by other authors [24,27]. It must be taken into account that the interface could catalyze the crystallization of the droplets. The effects of the substrate were clearly identified by Barham et al. [29] for precipitated PE droplets, resulting in different values for 'homogeneous' nucleation varying between 60 and 120 °C depending on the type of cover glass used for following the crystallization behavior with the optical microscope. Koutsky et al. [27] found for droplets dispersed in oil, that the crystallization was probably initiated at the oil-polymer melt interface. In these cases, the low temperature crystallization is not a volume dependent process (described by Eq. (5), but a heterogeneous surface dependent process, described by:

$$N/N_0 = \exp(-IAt) \tag{6}$$

where I is the nucleation rate expressed in number of nuclei per unit area and time, and A is the average area of the droplets.

These authors have shown that the crystallization that occurs at high supercooling has a nucleation rate which scales with the volume of the domain, indicating a volume dependent homogeneous process, instead of a surface-nucleated process. Due to the complexity of the blend system studied here and the increasing polydispersity of the samples at higher PA6 concentrations, we are unable to produce a statistically significant plot of nucleation rate versus droplet volume or droplet surface via isothermal DSC experiments. However, there are strong indications that in the (PS/SMA2)/PA6 blend systems, nucleation was probably initiated at the interface. In Fig. 6, it can be seen that the homogeneous nucleation temperature ($T_{c,peak}$) for the PA6 in the (PS/SMA2)/PA6 blends is consequently 4–6 °C higher for equal droplet sizes than in case of the (PPE/PS/SMA2)/PA6 blends. This cannot be caused by a change in interfacial tension of the system, because both blend systems are expected to have very similar values [36]. It can also not be explained by differences in blend morphology, as all blend compositions exhibit quite monodispers phase morphologies, with spherical droplets (see Table 2, and SEM pictures given in [6]). Both systems also contain quite similar amounts of SMA compatibilizer. The most likely explanation is that it has to be attributed to the vitrification of the PS matrix phase, which has a glass-transition temperature very close to the onset of the homogeneous nucleation peak. Differences in thermal expansion of matrix and dispersed component, can lead to pressure differences, inducing nucleation of the PA6 phase. In a number of recent papers, it was found that vitrification of the amorphous polymer matrix could strongly increase the PA6 nucleation density around the vitrification temperature of the matrix [4–6]. This aspect needs further investigation to be solved completely. As such, we conclude that the PA6 droplet crystallization in the range 85–100 °C in the (PS/SMA2)/PA6 blends could be initiated at the interface, even though a random nucleation mechanism is observed.

Another factor influencing the nucleation rate in the (PS/SMA2)/PA6 blends investigated here, could be the presence of the SMA compatibilizer. The reaction of SMA with PA6 has been found to affect the PA6 crystallization rate in bulk PA6 at high enough SMA concentrations and can likely cause restrictions on PA6 chain mobility, decreasing the (homogeneous) nucleation rate. The smaller PA6 droplet size together with the disturbing effect of the SMA2 compatibilizer likely causes the much lower homogeneous nucleation temperature (40 °C lower found here) compared to the experiments of Koutsky et al. performed on 1–2 μm sized PA6 droplets [27].

3.3. Crystallinity of (sub)-micrometer-sized PA6 droplets as determined with DSC

3.3.1. Crystallinities of PA6 in PS/PA6 blends at intermediate supercooling

In Fig. 7 the crystallinities of the PA6 droplets for different PS/PA6 blends are plotted as a function of the volume average droplet size. The crystallinities were determined using DSC both in cooling and heating, taking into account the temperature dependent enthalpies,

calculated from data in the ATHAS databank for PA6 (Eqs. (1) and (2)). It is seen that the PA6 crystallinity determined from the crystallization peaks equals the one determined from the melting data (after correction for crystallization during heating). The crystallinity of the PA6 droplets clearly decreases with decreasing droplet size. Included are DSC crystallinity data of some PS/PA6 blend compositions, obtained after applying a self-nucleation treatment. This self-nucleation treatment drastically increases the number of heterogeneous nuclei, resulting in a full reintroduction of crystallization at the bulk temperature of PA6 (see [5]). These nucleated blends still show a decrease of crystallinity with decreasing droplet size, indicating the importance of the confinement of the micrometer-sized PA6 droplets on the crystallization phenomena. The observed crystallinity decrease with smaller droplet size is most likely reflecting the increasing disturbing effect of the small volume the polymer is confined to. It can also possibly be related to the lower growth rate for smaller droplets at intermediate crystallization temperatures (see [5]), which can result in a lower crystallinity obtained after a certain crystallization time. Lowering the DSC cooling rate, however, does not affect the trend obtained in Fig. 7 and only causes a slight increase in PA6 crystallinity (see data point in Fig. 7), which seems to exclude the latter explanation.

3.3.2. Crystallinities of PA6 in (PS/SMA2)/PA6 blends at high supercoolings

In Fig. 8 the DSC crystallinity is plotted as a function of the weight fraction of PA6 in the blend for the reactively compatibilized (PS/SMA2)/PA6 blends. The crystallinity is determined both from the cooling run (▼) and from the heating run (■) after taking into account the temperature dependence of the transition enthalpy (see Eq. (2), in cooling $T=85$ °C and in melting $T=220$ °C were taken). The crystallinity determined from the cooling run shows a very strong drop as soon as the sub-micrometer PA6 droplets are formed. The PA6 crystallinity decreases from ~30–35% for the bulk to ~10–15% in the sub-micrometer PA6 droplets. Besides the effect of the limited droplet size on the lateral dimensions, the crystallization temperature can also be important. Barham et al. [29] stated that the high nucleation densities in the supercooled PE droplets caused a hindrance for lateral growth, because of crowding at the crystallite surfaces, resulting in the formation of small and highly imperfect crystalline structures. Hoffmann and Weeks [51] reported catastrophic nucleation behavior resulting in the formation of extremely small folded chain crystals when polychlorotrifluoroethylene was crystallized at a supercooling of 70 °C or higher, assigned to homogeneous nucleation. It can be noticed that the drop in crystallinity coincides with the transition from a heterogeneous to a homogeneous nucleation process. The crystallinity is not strongly dependent on the droplet size (the droplet sizes decrease from ~0.5 to 0.1 μm for the blends shown), which seems to indicate that the largest contribution to the crystallinity decrease in these blends is caused by the effect of the crystallization temperature and to a lesser extent by the size of the droplets. The direct effect of the compatibilizer on the crystallinity (see previous results [6] which indicated a decrease in crystallinity of PA6 upon reaction with SMA compatibilizer) can most likely be neglected, because of the relatively low concentration of SMA2 reacted at the interface for the considered blends.

Obviously, a clear discrepancy is observed between these crystallinities compared to those determined from the melting run. For PA6 droplets crystallizing at intermediate crystallization temperatures, an analogous- though smaller—effect could be corrected for, see Section 3.3.1 (see Fig. 7). The observed discrepancy is most likely that strong because of imperfect crystallization at low temperatures,

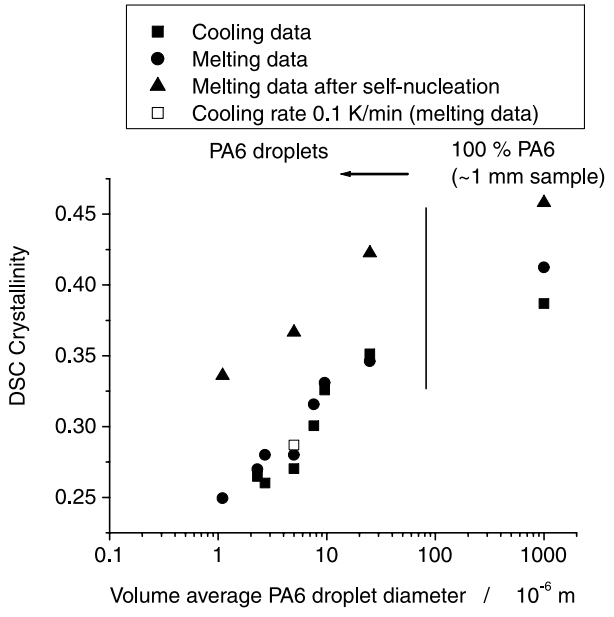

Fig. 7. DSC crystallinity as a function of the PA6 droplet size in PS/PA6 and (PPE/PS)/PA6 blends.

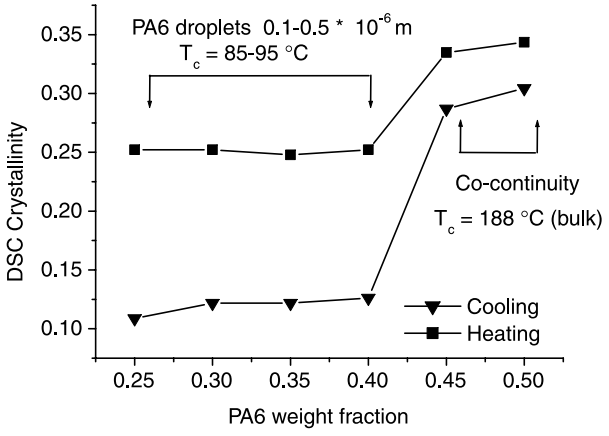

Fig. 8. Evolution of DSC crystallinity from cooling (▼) and melting curves (■) versus PA6 droplet size for various (PS/SMA2)/PA6 blend compositions.

followed by reorganization of the crystallites formed and further crystallization in the subsequent heating run, resulting in a higher melting enthalpy. Reorganization could include perfectioning and thickening of crystallites, while at high temperatures also the lateral dimensions could increase by additional crystallization. It can be expected that the correction method used for determination of the kinetic data presented in Fig. 4, is not completely sufficient to correct for this large scale reorganization of PA6 crystallites during heating. However, the amount of reorganization can be expected to be directly dependent on the number of droplets that has crystallized (i.e. every crystallized droplet will reorganize very fast during heating), so the increase in enthalpy with respect to any further reorganization can be considered as a simple multiplication factor to the data presented in Fig. 4, and thus most likely does not modify the conclusions presented there. Strong improvements of crystalline order in heating via DSC were also observed for PEO crystals in nano compartments of 12 nm in PB_h-b-PEO block copolymers [22,50]. A broad melting range was observed related to the superposition of sharp melting transitions of the individual crystals, which take place at different temperatures corresponding to a multitude of possible metastable states. Stabilization by reorganization was found to take place entirely in the crystalline state: melting-recrystallization processes were inhibited in the small cells [50].

4. Conclusions

It has been shown that the crystallization kinetics of PA6 in immiscible blends of PS/PA6 and (PS/SMA2)/PA6 blends can be studied over a very broad temperature range, without the need of using high cooling rates. For immiscible PS/PA6 blends with PA6 droplets of micrometer size, exhibiting only a moderate decrease of crystallization temperature compared to the PA6 bulk crystallization, an athermal nucleation mechanism is suggested based on a nucleation process which takes place in a very small temperature interval.

For the (PS/SMA2)/PA6 blends with submicrometer-sized PA6 droplets, crystallizing at very low temperature around 90 °C (supercoolings of approximately 100 °C compared to $T_{c,bulk}$), a random nucleation event was found using isothermal DSC experiments, which is characteristic of a homogeneous nucleation process. Interestingly, the effects were found up to high concentrations of the dispersed phase, i.e. 40 wt% PA6, which is, to the best of our knowledge, the highest concentrated heterogeneous system reported, exhibiting homogeneous nucleation kinetics. The nucleation rate at the very low temperatures was strongly temperature dependent and was also found to decrease with decreasing PA6 droplet size. However, the nucleation of these PA6 droplets was believed to be initiated at the blend interface, due to vitrification of the PS matrix component close to the onset of the low temperature crystallization peak as indicated by DSC, so no true homogeneous volume process is observed.

Besides crystallization temperatures also the final PA6 crystallinities were strongly affected by the confining conditions of the droplets. For 1–30 μm sized PA6 droplets crystallizing at intermediate temperatures, the crystallinity decreased with decreasing PA6 droplet size from 36% for bulk PA6 down to 22%. For the sub-micrometer sized PA6 droplets, a very strong decrease in crystallinity was found down to 10%. As a result of the low crystallization temperatures, very imperfect crystals are formed, leading to strong reorganization during subsequent heating.

Acknowledgements

The authors are indebted to the Research Fund of the KULeuven (GOA 98/06), and to the Fund for Scientific Research-Flanders, Belgium for the financial support given to the MSC-laboratory.

References

[1] Frensch H, Harnischfeger P, Jungnickel BJ. In: Utracki LA, Weiss RA, editors. ACS Symposium Series, 395, 1989. p. 101.
[2] Santana OO, Müller AJ. Polym Bull 1994;32(4):471.
[3] Arnal ML, Matos ME, Morales RA, Santana OO, Müller AJ. Macromol Chem Phys 1998;199(10):2275.
[4] Everaert V, Groeninckx G, Aerts L. Polymer 2000;41:1409.
[5] Tol RT, Mathot VBF, Groeninckx G. Confined Crystallization phenomena in immiscible polymer blends with dispersed micro- and nanometer sized pa6 droplets, part 1: uncompatibilized PS/PA6, (PPE/PS)/PA6 and PPE/PA6 blends. Polymer 2005;46(2):369.
[6] Tol RT, Mathot VBF, Groeninckx G. Confined Crystallization phenomena in immiscibllle polymer blends with dispersed micro- and nanometer sized pa6 droplets, part 2: reactively compatiblized PS/PA6 and (PPE/PS)/PA6. Polymer 2005;46(2):383.
[7] Groeninckx G, Vanneste M, Everaert V. In: Utracki LA, editor. Polymer blends handbook. Crystallization, morphological structure and melting of polymer blends, vol. 1. Chapter 3.
[8] Turnbull D. J Appl Phys 1950;21:1022.
[9] Turnbull D, Cormia RL. J Chem Phys 1961;34:820.
[10] Montenegro R, Antonietti M, Mastai Y, Landfester K. J Phys Chem B 2003;107:5088.
[11] Vonnegut B. J Colloid Sci 1948;3:563.
[12] Turnbull D. J Chem Phys 1952;20:411.
[13] Lotz B, Kovacs AJ. ACS Polym Prepr, Div Polym Chem 1969;10(2): 820.
[14] O'Malley JJ, Crystal RG, Erhardt PF. ACS Polym Prepr, Div Polym Chem 1969;10(2):796.
[15] Robitaille C, Prudhomme J. Macromolecules 1983;16:665.
[16] Loo Y-L, Register RA, Ryan AJ. Phys Rev Lett 2000;84(18):4120.
[17] Loo Y-L, Register RA, Ryan AJ, Dee GT. Macromolecules 2001;34: 8968.
[18] Xu J-T, Fairclough PA, Mai S-M, Ryan AJ, Chaibundit C. Macromolecules 2002;35:6937.
[19] Lee W, Chen HL, Lin TL. J Polym Sci Part B: Polym Phys 2002; 40(6):519.
[20] Müller AJ, Balsamo V, Arnal ML, Jakob T, Schmalz H, Abetz V. Macromolecules 2002;35(8):3048.

[21] Müller AJ, Arnal ML, Lopez-Carrasquero F. Macromol Symp 2002; 183:199.
[22] Reiter G, Castelein G, Sommer J-U, Röttele A, Thurn-Albrecht T. Phys Rev Lett 2001;87(22):226101.
[23] Massa MW, Carvalho JL, Dalnoki-Veress K. Eur J Phys E 2003; 12(1):111.
[24] Cormia RL, Price FP, Turnbull D. J Chem Phys 1962;37(6):1333.
[25] Burns JR, Turnbull D. J Appl Phys 1966;37(11):4021.
[26] Gornick F, Ross GS, Frolen LJ. ACS Polym Prepr, Div Polym Chem 1966;7:82.
[27] Koutsky JA, Walton AG, Baer E. J Appl Phys 1967;38(4):1832.
[28] Burns JR, Turnbull D. J Polym Sci 1968;6(A2):775.
[29] Barham PJ, Jarvis DA, Keller A. J Polym Sci Phys Ed 1982;20:1733.
[30] Ghysels A, Groesbeek N, Yip CW. Polymer 1982;23:1913.
[31] Perepezko JH, Höckel PG, Paik JS. Thermochimica Acta 2002;388: 129.
[32] Aref-Azar A, Hay JN, Marsden BJ, Walker N. J Polym Sci Phys Ed 1980;18:637.
[33] Sanchez A, Rosales C, Laredo E, Müller AJ, Pracella M. Makromol Chem Phys 2001;202:2461.
[34] Everaert V, Groeninckx G, Koch MHJ, Reynaers H. Polymer 2003; 44(12):3489.
[35] Tol RT, Groeninckx G, Vinckier I, Moldenaers P, Mewis J. Polymer 2004;45:2587.
[36] Everaert V, Groeninckx G, Pionteck J, Favis BD, Aerts L, Moldenaers P, et al. Polymer 2000;41:1011.
[37] Fried JR, Hanna GA. Polym Eng Sci 1982;22:705.
[38] Wittler H, Leiser G, Drosher M. Makromol Chem Rapid Commun 1993;14:401.
[39] ATHAS data bank. http://web.utk.edu/~athas/databank. For a description see: Wunderlich B. Pure Appl Chem 1995;67:1019.
[40] Wunderlich B. Macromolecular physics. Crystal melting. vol. 3. New York: Academic Press; 1980.
[41] Illers K-H. Makromol Chem 1978;179:497.
[42] Blundell DJ, Keller A, Kovacs AJ. J Polym Sci 1966;B(4):481.
[43] Wunderlich B. Macromolecular physics. Crystal nucleation-growth-annealing. vol. 2. New York: Academic Press; 1976.
[44] Janeschitz-Kriegl H, Ratajski E, Wippel H. Colloid Polym Sci 1999; 277(2–3):217.
[45] Gandica A, Magill JH. Polymer 1972;13:595.
[46] Burnett BB, McDevit WF. J Appl Phys 1957;28:1101.
[47] Hoffmann JD. Polymer 1983;24:3.
[48] Turnbull D, Fischer JC. J Chem Phys 1949;17:71.
[49] Massa MV, Dalnoki-Veress K. Phys Rev Lett 2004;92(25). 2555091/-255509/4.
[50] Rottele A, Thurn-Albrecht T, Sommer JU, Reiter G. Macromolecules 2003;36(4):1257.
[51] Hoffmann JD, Weeks JJ. J Chem Phys 1962;37:1723.